Khan et al., J Material Sci Eng 2018, 7:5
DOI: 10.4172/2169-0022.1000490

Journal of Material Sciences & Engineering

Research Article | Open Access

Towards Understanding Citric Acid Derived High Quantum Yield Molecular Fluorophores: From Carbon Dots to Spherical Organic Nanocrystals

Syamantak Khan, Sanjhal Jain and Chayan K Nandi*

School of Basic Sciences, Indian Institute of Technology, Mandi, Himachal Pradesh, India

Abstract

The origin of the multicolor emission in carbon dots (C-dots) is still debatable. Recently molecular fluorophore found to be one of the main components during the synthesis of C-dots. Even, this molecular fluorophore may give rise to the C-dots like structure under transmission electron microscope (TEM) in a drying mediated process. Here, we show that pH dependent protonated and deprotonated species of these small molecular fluorophores can give rise to spectral heterogeneity and excitation-dependent emission spectra in a solution, similar to C-dots. Using fluorescence correlation spectroscopy and time-resolved anisotropy, we reveal that their hydrodynamic size matches with the molecular fluorophores in solution phase. This size obtained is much smaller than the size of C-dots suggesting that the bigger nanocrystals observed under TEM is actually the aggregated structure of this molecular fluorophore. This study suggests that, C-dots, especially synthesized from citric acid should be studied carefully for the future applications.

Keywords: Carbon dots; High quantum yield; Protonation-deprotonation reaction; pH dependence photoluminescence; Time-resolved fluorescence; Anisotropy decay

Introduction

Facile and large-scale synthesis of low-cost photoluminescent materials has always been a widespread research interest. Citric acid is one of the commonly studied precursors to synthesize high quantum yield fluorescent materials. The ability of citric acid to form fluorescent citrazinic acid by condensation reaction is known from the last century [1]. Yet, it was observed only recently that some derivatives of citrazinic acid can have very high fluorescence quantum yield. Kasprzyk et al. reported a series of novel fluorescent compounds from condensation mixtures of citric acid and specific β-amines [2]. These com-pounds consisted of five-membered ring fused 2-pyridones and exhibited quantum yields as high as 79%. Interestingly, recent studies reported the synthesis of fluorescent carbon dots (C-dots) and graphene quantum dots (GQD) using hydrothermal or pyrolysis based synthesis methods from citric acid with very high quantum yield (QY) up to 90% [3-5]. Now, in the light of other carbon nanostructures like fullerene, nanotube or graphene, such bright photoluminescence is unlikely to originate from carbon. Although heteroatom doping of these C-dots with nitrogen and sulfur has been reported as a plausible explanation for the increased QY [5-7], it put a question mark whether such high QY is observed from carbon at all or originates from molecular fluorophores. Yet, the potential of these materials remains irrefutable, especially as they are very bright and their synthesis is easy to scale up with a very low cost [7,8].

Some recent studies report on molecular like fluorophore in C-dots [2,7,9-12], although with some anomalous observations. Temperature-dependent carbonization process from highly fluorescent fluorophore (created at low temperature in the initial stage to less fluorescent C-dots) is reported [11,13]. Few reports suggest that the molecular fluorophores are attached to the surface of the C-dots with multi-emissive states like core, surface and edge states, which is responsible for the fluorescence [14-17]. On the other hand, the presence of free fluorophore along with C-dots has also been proposed [9,10], in contrast to the concept of the core, surface and edge states. Also, these free fluorophores show closely similar pH-dependent optical changes to C-dots. The excitation dependent multicolor fluorescence of some fluorophores was observed for a particular pH, below or above which the excitation-dependent multicolor fluorescence disappears [3]. This led us to the important hypothesis on the presence of protonated-deprotonated species of the fluorophore in the solution that may guide the observed excitation dependent multicolor emission in a pH-dependent manner [3,18]. As a result, the pH-dependent studies of these systems could be pivotal to understand their mechanism of photoluminescence at the molecular level. Here, we have elucidated the mechanism of pH-dependent optical changes of a very high QY fluorophore (~70%) namely 5-oxo-3,5-dihydro-2H-thiazolo [3,2-a]pyridine-3,7-dicarboxylic acid (TPDCA). The crystal structure of TPDCA recently has been reported by Shi et al. [9]. Initially it was reported as high QY sulfur and nitrogen doped C-dots (N,S-C-dots) [5]. We extended our work for another nitrogen doped C-dots (N-C-dots), that has the highest reported QY (~94%) till date [3]. Based on the similarities in the reaction mechanism (Figure S1) and the new experimental results provided here, we propose that N-C-dots is also contain small molecular fluorophore (like TPDCA) which govern the fluorescence proper-ties of the system. This is named as OPCA (3,5-dihydro-3,3-bis(hydroxymethyl)-5-oxo-2H-oxazol[3,2-a] pyridine-7-carboxylic acid (OPCA). Therefore throughout the manuscript, we refer this material as OPCA instead of N-C-dots.

Synthesis and Characterization

TPDCA and OPCA were derived by condensation of an equimolar

***Corresponding author:** Chayan K Nandi, School of Basic Sciences, Indian Institute of Technology, Mandi, Himachal Pradesh, India, Tel: 01905-237917; E-mail: chayan@iitmandi.ac.in

Received October 08, 2018; **Accepted** October 09, 2018; **Published** October 19, 2018

Citation: Khan S, Jain S, Nandi CK (2018) Towards Understanding Citric Acid Derived High Quantum Yield Molecular Fluorophores: From Carbon Dots to Spherical Organic Nanocrystals. J Material Sci Eng 7: 490. doi: 10.4172/2169-0022.1000490

ratio of citric acid with β-amino thi-ols (L-cystine) or β-amino alcohol (trisaminomethane or TRIS) at 150°C in an oven for 2 hours. The high quality purified fluorophores were extracted out from the product mixture by crystallization using water as a solvent. Single crystal XRD confirmed the chemical structures. ^{1}H and ^{13}C nuclear magnetic resonance spectroscopy (NMR) and the molecular mass were confirmed by High-Resolution Mass spectroscopy (HRMS) (Figure S2-S4). The high QY of TPDCA (~60%) and OPCA (~70%) was verified using a large 150 mm integrating sphere (Quanta–φ, HORIBA).

It is interesting to note that the chemical structures of TPDCA and OPCA show remarkable similarities, especially with a six-member aromatic ring (Figure 1) and a conjugated carboxylic acid group. It is worth mentioning that all the experimental data presented in this manuscript were performed by dissolving the pure crystals back into the water.

Results and Discussions

A very close similarity was observed in the UV-Vis absorption spectra between TPDCA and OPCA. The peak at around 330-350 nm and at around 240 nm are designated as n-π* and π-π* transitions (Figure S5). However, for these strongly conjugated and donor-acceptor substituted molecules, the transition corresponding to 330-350 nm can also be π-π*. Nevertheless, these are the commonly observed molecular fluorophore like signature while many of the earlier reports attributed them to the edge and core states absorption of C-dots [14-17]. Both the molecules hardly show any change in the absorption or emission spectra in water at neutral pH or higher pH, however, a systematic red-shift both in the absorption and emission spectra for both TPDCA and OPCA was observed when pH of the solution was gradually decreased (Figure 2a-2d). This contrasting observation suggests the important role of protonation-deprotonation reactions of the carboxylic acid groups and thus producing multiple species (COOH and COO-). A critical analysis of pH-dependent spectral shifting (Figure 2e and 2f) shows that the change in absorption and emission maxima is highly correlated with the protonation and deprotonation kinetics of TPDCA and OPCA. From the dissociation kinetics (Figure 2e and 2f) an estimated pKa in between 5-7 for TPDCA and in between 2-3 for OPCA was calculated. A recent study [19] on pH-dependent fluorescence change of graphene oxide functionalized with COOH, OH and NH_2 showed three pKa values at 4.3, 6.6 and 9.8. These were designated as dissociation of carboxylic acid in the presence of hydroxyl group, isolated carboxylic acid and phenolic OH group respectively.

Hence the comparison of the pKa in between 5-7 actively support the dissociation kinetics of only car-boxylic acid in TPDCA, whereas the much lower pKa value in OPCA suggested the dissociation kinetics of carboxylic acid in the vicinity of OH group in the molecule. It is predictable that protonation and deprotonation kinetics of the conjugated carboxylic acid will affect the conjugation energy of the aromatic ring. However, it is often observed that transition energies of $(\text{-R-COO}^{--}) \rightarrow (\text{R-COO}^{--})^{*}$ are high-er than $(\text{-R-COOH}) \rightarrow (\text{-R-COOH})^{*}$ [20]. Here one reason could be that protonated TPDCA or OPCA are prone to exist in a dimer form which leads to excess energy stabilization. A deprotonated carboxyl group loses the capability of hydrogen bonding and in turn, possess increased energy gap between the ground and excited state. This explains the above observed spectral changes. Interestingly, a recent study reports just the opposite trends of the spectral changes, where a spectral blue shift in both the absorption and emission spectra were observed with decreasing pH [18]. The pKa value was also obtained as 7.9, which strongly support phenol-phenolate equilibrium responsible for their spectral changes. As a result, it is quite obvious that the type and the predominance of the

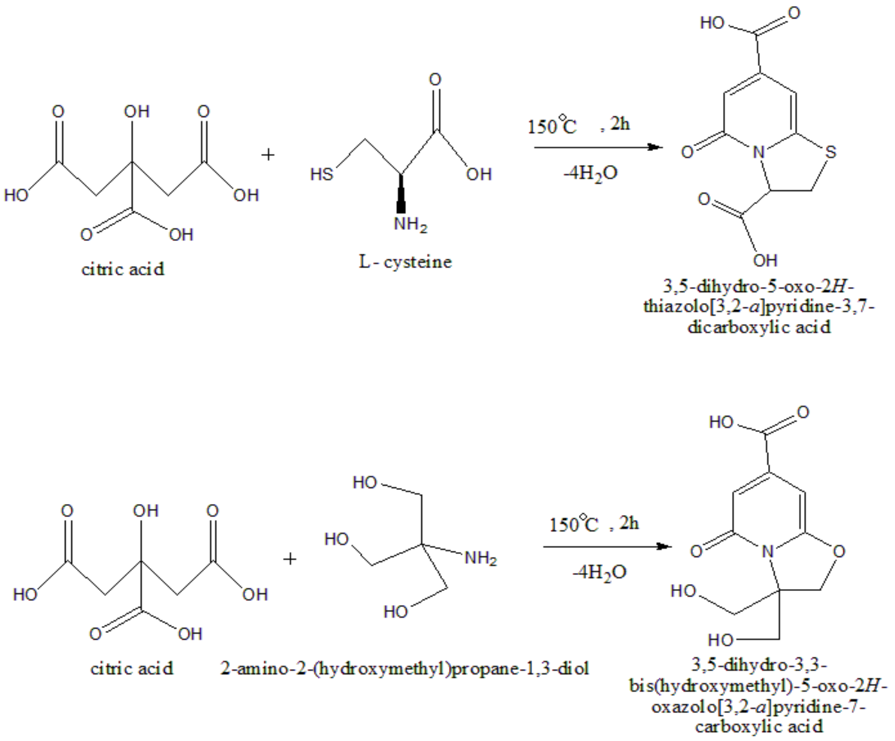

Figure 1: Formation mechanism of TPDCA and OPCA via condensation reaction.

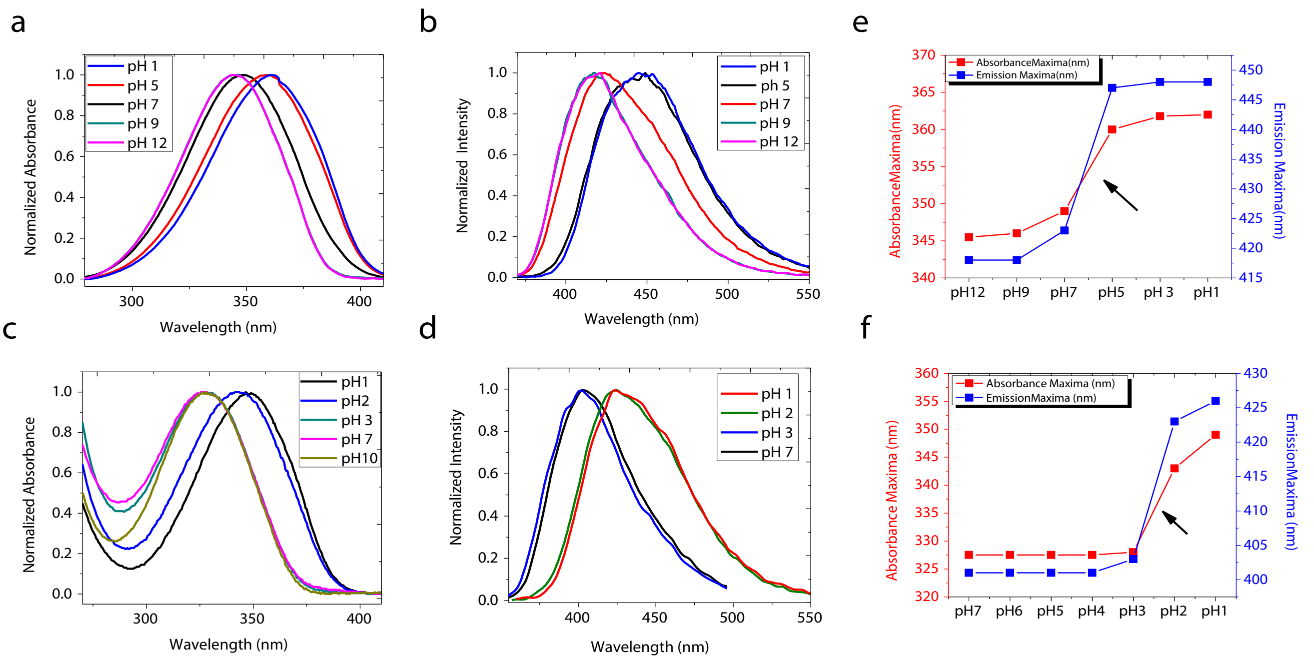

Figure 2: (a) Absorption and (b) emission spectra of TPDCA and. (c) Absorption and (d) emission spectra of OPCA. (e and f) Analysis of spectral shift of TPDCA and OPCA, respectively (red is absorption and blue is emission).

functional group (COOH, OH or NH_2, etc.) determine the dissociation kinetics and eventually the spectral changes.

It is to be noted here that the normalized absorption and emission spectra of TPDCA and OPCA show higher full-width half maxima (FWHM) at low pH compared to the higher pH. An approximately 10 nm increase (~250 cm^{-1}) of FWHM in the absorption, as well as emission spectra of both TPDCA and OPCA, was observed. This could be a result of two different factors. At low pH, the protonated species can form intermolecular hydrogen bonds, which lead to the vibrational coupling of –COOH groups in dimeric or multimeric form. This is a ubiquitous feature in hydrogen-bonded carboxylic acid systems [21]. Secondly, broadening can also arise from spectral heterogeneity, i.e. presence of two closely emissive species. This spectral heterogeneity was further elucidated with time-resolved emission spectroscopy (TRES). The TRES is a powerful technique to identify multiple emissive excited states. Time-resolved area normalized emission spectra (TRANES) is a unique analysis of TRES where a number of emissive species can be identified accurately [22,23]. A useful feature of TRANES is that an isoemissive point in the spectra supports any model that involves multiple emitting species in the sample. The isoemissive point in TRANES exists for all cases in which two emissive species are kinetically coupled either irreversibly or reversibly or not coupled at all [22,23]. The pH-dependent TRES (Figure S6 and S7) and TRANES spectra (Figure 3a-3d) shows that multiple emissive states arise mostly in between pH5-pH7 due to the carboxylic acid -carboxylate equilibrium. The emission maximum at 414 nm (pH 9, Figure 3b) found to be gradually red-shifted to 440 nm (pH 1, Figure 3a) with decreasing pH. Interestingly, in pH5-pH7 spectral migration occurs through a single isoemissive point at 430 nm (Figure 3a). With an analogy of isosbestic point in UV-Visible absorbance spectra, isoemissive point in TRANES indicates a wave-length where the emission of normalized spectra remains unchanged with time. It also proves that there exist only two emissive species and no intermediate in between. This isoemissive point at 430 nm also manifests in the intersection of two steady state spectra at two extreme pH conditions (Figure 2b). Exact similar results were also obtained from OPCA (Figure 3c and 3d) where the isoemissive point at 415 nm is visible in the steady-state spectra (Figure 2d). At higher pH, TRANES shows single emissive state which is attributed to the complete deprotonation of the carboxyl groups. So here we conclude that spectral heterogeneity of both in TPDCA and OPCA molecule arise from two kinetically coupled emissive species and therefore cannot be physically separated from each other by analytical methods.

To further elucidate the actual size of the emitters in solution, we performed fluorescence correlation spectroscopy (FCS) and time-resolved anisotropy (TRA) measurements. It is well known that, the translational and rotation diffusion speed of an emitter in the solution is strongly correlated with its hydrodynamic volume. The relation between the hydrodynamic radius (r) and the translational diffusion speed, commonly known as the diffusion coefficient (D), is given by the Stokes-Einstein equation (eqn. (1)). Similarly, the relationship between the volume (V) of the emitter and the rotational correlation time (θ), is given by the Perrins equation (eqn. (2))

$$D = \frac{k_B T}{6\pi\eta r} \qquad (1)$$

$$\theta = \frac{V\eta}{k_B T} \qquad (2)$$

Where k_B is Boltzmann constant, T is temperature and η is the viscosity of the medium [24]. FCS is a nearly single molecule fluorescence fluctuation based powerful technique to directly probe the translational diffusion coefficient with high accuracy [25]. The fluorescence fluctuation is measured and an autocorrelation curve is generated to determine the diffusion coefficient. Finally, the hydrodynamic diameter (D_H) and the actual size of the emitter are calculated using

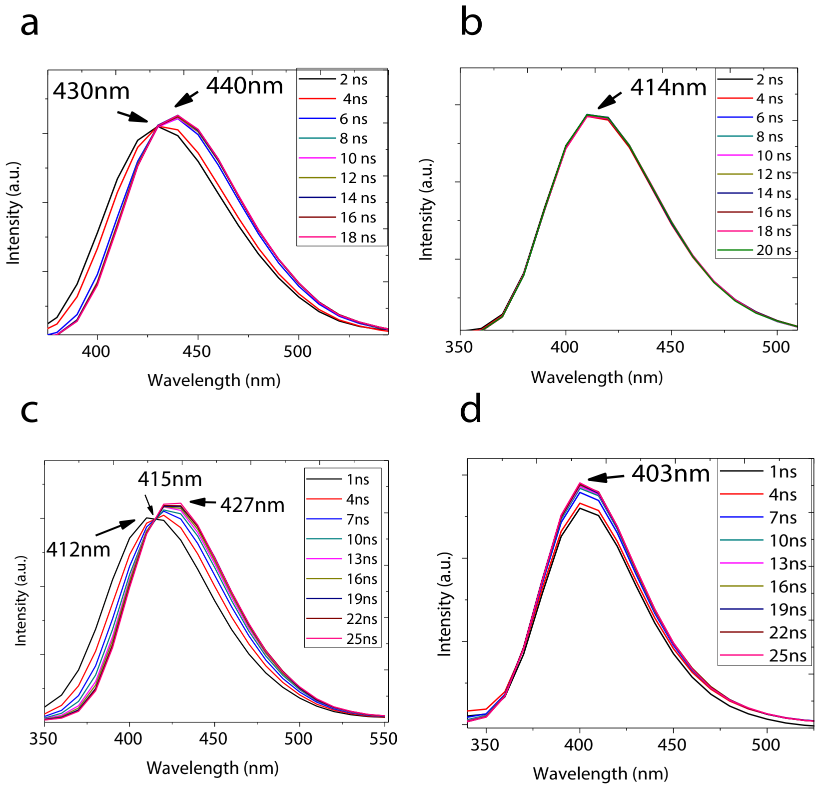

Figure 3: TRANES spectra of TPDCA and OPCA at different pH conditions (a and b) TRANES spectra of TPDCA at pH 5 and pH 9 respectively. (a) Spectral migration through an isoemissive point at 430 nm is observed in acidic pH. The emission maxima shift around 10 nm in the first 20 ns of emission. (c and d) TRANES spectra of OPCA at pH 5 and pH 9 respectively. (c) Spectral migration through an isoemissive point at 415 nm is observed in acidic pH. The emission maxima shift around 15 nm in the first 20 ns of emission.

Stokes Einstein equation (eqn. (1)). The FCS measurements were done by calibrating the diffusion volume with a standard fluorophore (Atto488, Diffusion coefficient=400 ± 50 $\mu m^2/s$) [26]. Figure 4a shows autocorrelation curve at a neutral pH (deprotonated species) of TPDCA and OPCA. The normalized autocorrelation curves of TPDCA and OPCA (inset) are found to be nearly overlapping. The diffusion coefficient was found to be 358 ± 35 $\mu m^2/s$ which is very close to Atto488 (a dye used for calibration) confirming the small size ($D_H \simeq 1$ nm) of the fluorescent materials both the cases. TRA decay Figure 4b of both TPDCA and OPCA also shows faster rotational dynamics (~0.5 ns) corresponding to small molecules.

To further verify the hydrodynamic size of the fluorescence emitters, we measured FCS and TRA in different pH conditions (Figure S8-S11). Figure 4c shows small increment of D with the decrease in pH, suggesting the formation of small hydrogen-bonded dimer or multimers of TPDCA and OPCA while denying the possibility of fluorophore aggregation in the dimension of the observed size in TEM (~3-5 nm). The rotational correlation time (θ) calculated from the pH dependent TRA measurements of both TPDCA and OPCA strongly support the FCS results (Figure 4d). The value found to be in the range of 500-650 ps both for TPDCA and OPCA at neutral pH strongly supports the small molecular fluorophore (comparable with Tryptophan=680 ps with MW=204 D which is almost two orders faster than the=20 ns in human serum albumin (HSA), MW=66 kD (Figure S12). A slight increase in the value with decreasing pH suggests the possible dimer or multimers formation. Therefore, both FCS and TRA decay measurements confirm that the emitters in both TPDCA and OPCA are molecular fluorophores. Thus our study takes a leap forward to resolve the central quest of structure-function relationship of C-dots.

Now, the contradictions between the molecules like optical properties and observation of carbon nanoparticles under transmission microscope (TEM) was needed to resolve. Interestingly, when we drop cast pure TPDCA solution on TEM grid, it shows a uniform distribution of nanoparticles with narrow size distribution and clear lattice fringes (Figures 5a and S13). Although apparently surprising, this observation was found to be consistent with few other di-carboxylic acids like malic acid and itaconic acid (Figure S14) confirming the pivotal role of the carboxyl group in strong hydrogen bonding and ordered aggregation process to form uniform sized nanocrystals. In a recent study, we have shown that itaconic acid or methylenesuccinic acid is produced in the hydrothermal treatment of citric acid, in a similar reaction condition which is commonly used for the synthesis of C-dots [27]. With a range of experimental techniques and quantum chemical calculations, we show that methylenesuccinic can give rise to hydro-gen-bonded nano-assemblies with C-dots-like properties and the lattice arrangement can be predicted from the single crystal XRD data. Similarly, here the lattice arrangement of the nanocrystals can also be predicted from the crystal structure of the TPDCA, which shows the hydrogen bonded nanocrystalline assembly of the monomeric unit with a unique fashion (Figure 5b). This understanding is crucial as it resolves the common fallacy in the previous studies. As citric acid provides abundant COOH groups as a precursor, most of the fluorophores synthesized from citric acid are likely to form similar nanocrystals during the drying process. Here, it is interesting to observe that although TPDCA has a monoclinic

Citation: Khan S, Jain S, Nandi CK (2018) Towards Understanding Citric Acid Derived High Quantum Yield Molecular Fluorophores: From Carbon Dots to Spherical Organic Nanocrystals. J Material Sci Eng 7: 490. doi: 10.4172/2169-0022.1000490

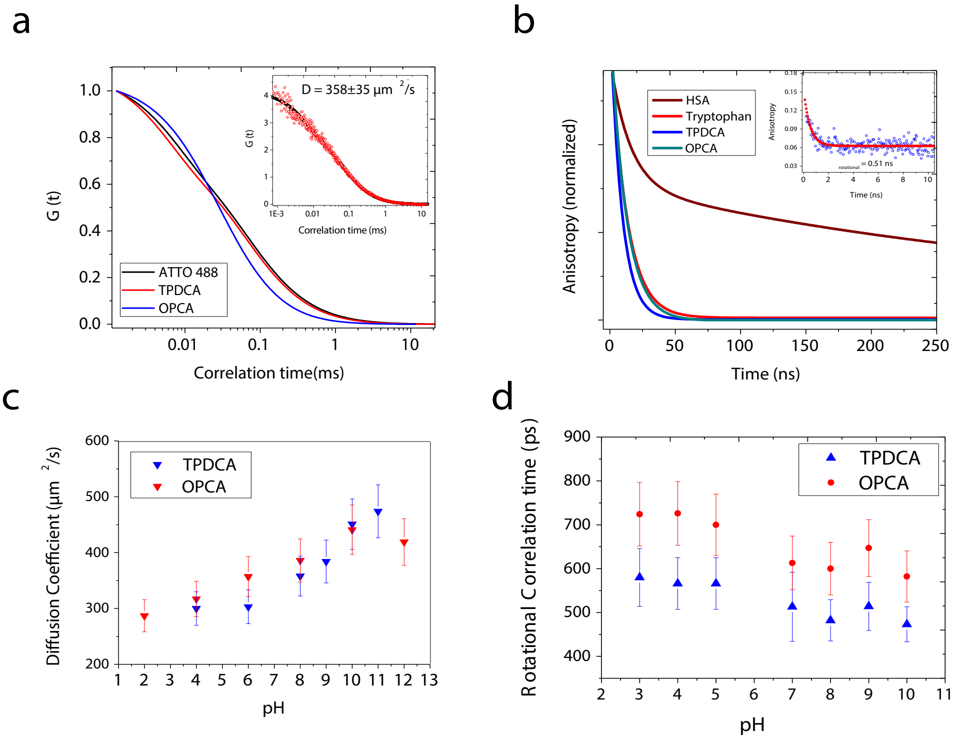

Figure 4: (a) Normalized fitted FCS autocorrelation curve of TPDCA, OPCA and Atto 488 shows a nearly overlapping pattern. Experimental data with diffusion fitting for TPDCA is shown in the inset. (b) Normalized TRA decay of TPDCA, OPCA, tryptophan and human serum albumin (HSA). (c) FCS measurements of TPDCA and OPCA at different pH conditions. (d) Measurement of rotational correlation time at different pH conditions.

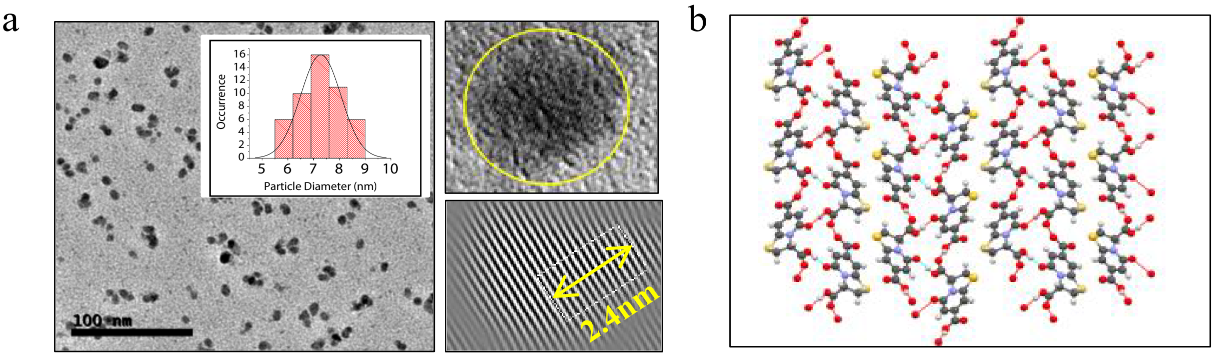

Figure 5: (a) Nanocrystals formed on the TEM grid during drop drying process. The nanocrystals have an average diameter of 7.5 nm (inset) and show crystallinity in HRTEM (right panel). Inverse FFT shows an average lattice spacing ($d_{h,k,l}$=0.24 nm) similar to graphitic carbon. (b) Hydrogen-bonded assembly of TPDCA as observed in the crystal structure.

crystal system, the nanocrystals again shows spherical morphology. A possible explanation could be the minimization of surface energy during the quick crystallization process [28]; however this needs to be con-firmed by further investigations. The data presented here certainly doesn't deny the formation of nanoparticle in solution when the reaction is carried with hydrothermal or pyrolysis synthesis. Instead, this study shows that the observed C-dots under TEM can also be the citric acid derived small fluorophores.

On the other hand, a large number of blue emissive C-dots and GQD which are reported till date show identical pH-dependent emission properties in the similar spectral range [3,15,18-20,29]. Few studies [15,29], using time-resolved techniques, observed multiple emissive states/species which actually give rise to the well-known complexity of C-dots photoluminescence. In those studies, the numbers of emissive states were also found to be strongly affected by pH of the solution. However, the exact mechanism by which multiple emissive states are created remained elusive. The origin of fluorescence in C-dots is generally attributed to surface functional groups like OH, COOH, NH_2, all of which exist in solution with a proton dissociation equilibrium. The current result provides evidence that emission properties of citric acid de-rived C-dots resembles very closely to fluorophores like TPDCA or OPCA. Our results also explain how the multi-emissive states can originate from two kinetically coupled emissive species.

Next, it is interesting to observe that the presence of two emissive states of these fluorophores can also give rise to excitation dependence emission spectra, which is very commonly observed in C-dots. Excitation dependence emission is one of the most debatable aspects of C-dots research till date. Previous studies, including ours, showed that excitation dependent red-shift could be controlled by controlling the polarity and pH of the solvent. We have also observed that the amount of inhomogeneous broadening or the number of emissive states, which were observed in time-resolved fluorescence, can be tailored by changing the pH of the solution [29,30]. In addition, our recent quantum chemical calculation on methyl-enesuccinic acid shows that presence of different ionic species and their dimers can cause spectral het-erogeneity. There also exist other evidences of spectral heterogeneity arising from small molecular species. Reckmeier et al. recently showed that aggregated fluorophores can cause multiple energy states and energy transfer between them [31]. This can mimic the emissive features of C-dots, i.e. core and surface state emission as reported by previous studies. Ehrat et al. showed that aromatic domains and molecular fluorophores exist in different proportions depending on the synthesis time of C-dots [31]. In their study, the blue emission was mostly found to be contributed by 2-pyridone derivatives which form at the early reaction stages, followed by the formation of aromatic domains which account for the emission from lower energy states. Here in this study, we show that the presence of two different emissive species, which exhibit spectral heterogeneity in TRANES, can cause of excitation dependent red-shifting of the emission spectra. This conclusion is very concordant with the recent observations by Choudhury et al. [18]. The study argues that the emissive species created by protonation of –OH is the key origin of excitation-dependent emission shift in C-dots. It is worth mentioning here that both TPDCA and OPCA show excitation-dependent emission properties only at lower pH conditions [3,9] (Figure S15). The spectra be-come stable, and excitation independent at higher pH, where all the carboxylic groups are entirely deprotonated and a single emissive species exist in the solution. It is already clear from previous discussions that both of the fluorophores contain two kinetically coupled emissive species (only in favorable pH) which have distinctly different absorption and emission maxima. The TRANES data both for TPDCA or OPCA suggested that at lower pH the longer wavelength species is more populated that the shorter wavelength, where at higher pH only shorter wavelength species is populated suggesting the longer wavelength species as protonated one. Therefore, when the excitation wavelength is shifted gradually to the lower energy, more and more protonated species are excited, resulting more emission from the protonated species, eventually giving rise to excitation-dependent emission properties. Additionally, fluorescence decay also causes a gradual decrease in emission intensity. In combination, they change the shape of the broadened spectra of the time-resolved measurements. A critical observation of the TRANES data with previous literature shows very close match of the results. This suggests that most of the previous studies with citric acid based C-dots [14-17] probably ended up with similar fluorophores.

Conclusions

In conclusion, small molecular fluorophores that govern the photoluminescence of citric acid derived C-dots, undergoes pH-dependent protonation-deprotonation reaction to produce multiple emissive species. The complex photoluminescence properties of citric acid derived C-dots stems from these multi-emissive species. These species gives rise to the excitation-dependent emission of the steady state spectra and spectral migration of the times resolved spectra. The heterogeneity arises from dissociation kinetics of the carboxyl functional group which creates different ionic emissive species. Moreover, in agreement with our previous study, these citric acid derived fluorophores produce spherical nanocrystals which look like carbogenic C-dot under HRTEM; however, they exist as small fluorescence emitter in the solution phase similar to common organic fluorophores. Thus, our study suggests that TPDCA, OPCA, and other similar ultra-bright organic fluorophores might have great potential in diverse applications. Hence, they should be researched further for their own merits, independently and separately from C-dots.

Supporting Information

The Supporting Information is available free of charge on the RSC Publications website. Detailed Experimental Section and Supporting Figures S1-S15 (PDF).

Acknowledgement

We acknowledge the AMRC facilities of IIT Mandi for our experiments and the Department of Biotechnology (Project No: BT/PR4067/BRB/10/1128/2012 for the financial support.

References

1. Sell WJ, Easterfield TH (1893) LXXIII.—Studies on citrazinic acid. Part I. Journal of the Chemical Society, Transactions 63: 1035-1051.
2. Kasprzyk W, Bednarz S, Żmudzki P, Galica M, Bogdał D (2015) Novel efficient fluorophores synthesized from citric acid. RSC Advances 5: 34795-34799.
3. Zheng C, An X, Gong J (2015) Novel pH sensitive N-doped carbon dots with both long fluorescence lifetime and high quantum yield. RSC Advances 5: 32319-32322.
4. Dong Y, Shao J, Chen C, Li H, Wang R, et al. (2012) Blue luminescent graphene quantum dots and graphene oxide prepared by tuning the carbonization degree of citric acid. Carbon 50: 4738-4743.
5. Dong Y, Pang H, Yang HB, Guo C, Shao J, et al. (2013) Carbon-based dots co-doped with nitrogen and sulfur for high quantum yield and excitation-independent emission. Angewandte Chemie 125: 7954-7958.
6. Sun D, Ban R, Zhang PH, Wu GH, Zhang JR, et al. (2013) Hair fiber as a precursor for synthesizing of sulfur-and nitrogen-co-doped carbon dots with tunable luminescence properties. Carbon 64: 424-434.
7. Zhang J, Yang L, Yuan Y, Jiang J, Yu SH (2016) One-pot gram-scale synthesis of nitrogen and sulfur embedded organic dots with distinctive fluorescence behaviors in free and aggregated states. Chemistry of Materials 28: 4367-4374.
8. Zhang J, Yu SH (2016) Carbon dots: large-scale synthesis, sensing and bioimaging. Materials Today 19: 382-393.
9. Shi L, Yang JH, Zeng HB, Chen YM, Yang SC, et al. (2016) Carbon dots with high fluorescence quantum yield: the fluorescence originates from organic fluorophores. Nanoscale 8: 14374-14378.
10. Schneider J, Reckmeier CJ, Xiong Y, von Seckendorff M, Susha AS, et al. (2017) Molecular fluorescence in citric acid-based carbon dots. The Journal of Physical Chemistry C 121: 2014-2022.
11. Song Y, Zhu S, Zhang S, Fu Y, Wang L, et al. (2015) Investigation from chemical structure to photoluminescent mechanism: a type of carbon dots from the pyrolysis of citric acid and an amine. Journal of Materials Chemistry C 3: 5976-5984.
12. Zhu S, Zhao X, Song Y, Lu S, Yang B (2016) Beyond bottom-up carbon nanodots: Citric-acid derived organic molecules. Nano Today 11: 128-132.
13. Krysmann MJ, Kelarakis A, Dallas P, Giannelis EP (2011) Formation mechanism of carbogenic nanoparticles with dual photoluminescence emission. Journal of the American Chemical Society 134: 747-750.
14. Reckmeier CJ, Wang Y, Zboril R, Rogach AL (2016) Influence of doping and temperature on solvatochromic shifts in optical spectra of carbon dots. The Journal of Physical Chemistry C 120: 10591-10604.
15. Dhenadhayalan N, Lin KC, Suresh R, Ramamurthy P (2016) Unravelling the multiple emissive states in citric-acid-derived carbon dots. The Journal of Physical Chemistry C 120: 1252-1261.
16. Ding H, Yu SB, Wei JS, Xiong HM (2015) Full-color light-emitting carbon dots with a surface-state-controlled luminescence mechanism. ACS nano 10: 484-491.

17. Sharma A, Gadly T, Neogy S, Ghosh SK, Kumbhakar M (2017) Molecular origin and self-assembly of fluorescent carbon nanodots in polar solvents. The journal of physical chemistry letters 8: 1044-1052.
18. Dutta Choudhury S, Chethodil JM, Gharat PM, Pal H (2017) pH-elicited luminescence functionalities of carbon dots: mechanistic insights. The Journal of Physical Chemistry Letters 8: 1389-1395.
19. Konkena B, Vasudevan S (2013) Spectral Migration of Fluorescence in Graphene Oxide Aqueous Dispersions: Evidence for Excited-State Proton Transfer. The journal of physical chemistry letters 5: 1-7.
20. Galande C, Mohite AD, Naumov AV, Gao W, Ci L, et al. (2011) Quasi-molecular fluorescence from graphene oxide. Scientific reports 1: 85.
21. Nandi CK, Chakraborty T (2004) Hydrogen bond-induced vibronic mode mixing in benzoic acid dimer: a laser-induced fluorescence study. The Journal of chemical physics 120: 8521-8527.
22. Koti ASR, Krishna MMG, Periasamy N (2001) Time-resolved area-normalized emission spectroscopy (TRANES): a novel method for confirming emission from two excited states. The Journal of Physical Chemistry A 105: 1767-1771.
23. Koti ASR, Periasamy N (2001) TRANES analysis of the fluorescence of nile red in organized molecular assemblies confirms emission from two species. Journal of Chemical Sciences 113: 157-163.
24. Lakowicz JR (1999) Fluorescence anisotropy. In Principles of fluorescence spectroscopy, Springer US pp: 291-319.
25. Röcker C, Pötzl M, Zhang F, Parak WJ, Nienhaus GU (2009) A quantitative fluorescence study of protein monolayer formation on colloidal nanoparticles. Nature nanotechnology 4: 577.
26. Kapusta P (2010) Absolute diffusion coefficients: compilation of reference data for FCS calibration. Application note 2.
27. Khan S, Sharma A, Ghoshal S, Jain S, Hazra MK, et al. (2018) Small molecular organic nanocrystals resemble carbon nanodots in terms of their properties. Chemical science 9: 175-180.
28. Golovin AA, Nepomnyashchy AA (2006) Self-Assembly, Pattern Formation and Growth Phenomena in Nano-Systems: Proceedings of the NATO Advanced Study Institute, held in St. Etienne de Tinee, France, August 28-September 11, 2004 (Vol. 218). Springer Science & Business Media.
29. Khan S, Gupta A, Verma NC, Nandi CK (2015) Time-resolved emission reveals ensemble of emissive states as the origin of multicolor fluorescence in carbon dots. Nano letters 15: 8300-8305.
30. Ehrat F, Bhattacharyya S, Schneider J, Löf A, Wyrwich R, et al. (2017) Tracking the source of carbon dot photoluminescence: aromatic domains versus molecular fluorophores. Nano letters 17: 7710-7716.
31. Reckmeier CJ, Schneider J, Xiong Y, Häusler J, Kasák P, et al. (2017) Aggregated Molecular Fluorophores in the Ammonothermal Synthesis of Carbon Dots. Chemistry of Materials 29: 10352-10361.